Reversible Anion Exchange and Catalytic Properties of Two Cationic Metal−Organic Frameworks Based on Cu(I) and Ag(I)

Honghan Fei, David L. Rogow, and Scott R. J. Oliver*

University of California, Santa Cruz, Department of Chemistry and Biochemistry, 1156 High Street, Santa Cruz, California 95064

Received March 12, 2010; E-mail: soliver@chemistry.ucsc.edu

Abstract: We report the synthesis and characterization of two Ag(I)/Cu(I)-based cationic metal−organic frameworks and their application in both heterogeneous catalysis and anion exchange. The Cu(I)-based material was designed from our previously reported Ag(I) cationic topology. Both structures consist of cationic layers with $\pi-\pi$ stacked chains of alternating metal and 4,4′-bipyridine. α,ω-Alkanedisulfonate serves as an anionic template, electrostatically bonding to the cationic layers. Due to weak interaction between the sulfonate template and cationic extended framework, both materials display reversible anion exchange for a variety of inorganic species. Indeed, the Ag(I)-based material exhibits highly efficient uptake of permanganate and perrhenate anion trapping, a model for pertechnetate trapping. The materials also display heterogeneous Lewis acidity, likely due to the coordinatively unsaturated metal sites which only bind to two bipy nitrogens and a weak interaction with one sulfonate oxygen. A comparative study on the influence of structure versus size selectivity and reusability for both exchange and catalysis is discussed.

Introduction

Anionic pollutants such as perchlorate (ClO_4^-), arsenate (AsO_4^{3-}), and chromate (CrO_4^-) are becoming increasingly problematic and are listed as EPA (U.S. Environmental Protection Agency) priority pollutants.[1] Perchlorate contamination of water by spent rocket fuel was reported in the lower Colorado River in 2002.[2] At the same time, organic anion pollution from pharmaceuticals—which are also intrinsically anionic—is now a worldwide problem, as most wastewater treatment ineffectively removes pharmacological anions.[3] Resins with cationic groups and exchangeable counteranions are still considered the standard ion exchanger.[4,5] These are of limited thermal and chemical stability, however, due to their organic polymer nature.[6] Layered double hydroxides (LDHs) are an isostructural group of structures based on brucite with a general formula $[M^{2+}_{1-x}M^{3+}_x(OH)_2]$-$A^n{}_{x/n} \cdot mH_2O$, where M^{2+} and M^{3+} are a range of metals (e.g., Mg^{2+} and Al^{3+}) and A^{n-} are interlamellar anions (e.g., CO_3^{2-}). They are considered to be an ideal alternative to anion exchange materials.[7] A variety of both inorganic and organic species are able to reversibly exchange into LDHs.[8−10] In many cases, however, the anion either cannot be removed or will deintercalate in the presence of common anions such as carbonate.[11−15] The need for materials qualified to trap or exchange both inorganic and organic anions remains. A recent development is a nanoporous cationic metal borate that on initial studies reversibly traps anions including pertechnetate, though the material is based on slightly radioactive thorium and anion removal percentage was 72%.[16]

New heterogeneous catalysts with greater reusability, efficiency, and ease of synthesis are continuously sought for environmental concerns. Micro/mesoporous materials have been extensively studied for their high internal surface area where the pore/channel catalytic sites lead to improved efficiency.[17] Microporous inorganic−organic hybrid materials with coordinatively unsaturated metal sites continue to be discovered, with Lewis acid catalytic properties.[18−20] There have been few systematic investigations, however, on the

(1) *Perchlorate environmental contamination: toxicological review and risk characterization*; Second external review draft, NCEA-1-0503; U.S. EPA, Office of Research and Development, National Center for Environmental Assessment, U.S. Government Printing Office: Washington, DC, 2002.
(2) Urbansky, E. T. *Environ. Sci. Pollut. Res. Int.* **2002**, *9*, 187–192.
(3) Castiglioni, S.; Bagnati, R.; Fanelli, R.; Pomati, F.; Calamari, D.; Zuccato, E. *Environ. Sci. Technol.* **2006**, *40*, 357–363.
(4) Praharaj, S.; Nath, S.; Panigrahi, S.; Ghosh, S. K.; Basu, S.; Pande, S.; Jana, S.; Pal, T. *Inorg. Chem.* **2006**, *45*, 1439–1441.
(5) Jana, S.; Praharaj, S.; Panigrahi, S.; Basu, S.; Pande, S.; Chang, C. H.; Pal, T. *Org. Lett.* **2007**, *9*, 2191–2193.
(6) Mark, R.; Findley, W. N. *Polym. Eng. Sci.* **1978**, *18*, 6–15.
(7) Slade, D. G. E. a. R. C. T. *Layered Double Hydroxides*; Duan, X., Evans, D. G., Eds.; Springer-Verlag: New York, 2006.
(8) Prasanna, S. V.; Kamath, P. V. *Solid State Sci.* **2008**, *10*, 260–266.
(9) Ma, R. Z.; Liu, Z. P.; Li, L.; Iyi, N.; Sasaki, T. *J. Mater. Chem.* **2006**, *16*, 3809–3813.
(10) Goh, K. H.; Lim, T. T.; Dong, Z. L. *Environ. Sci. Technol.* **2009**, *43*, 2537–2543.
(11) Chibwe, K.; Jones, W. *J. Chem. Soc., Chem. Commun.* **1989**, 926–927.
(12) Mackenzie, K. J. D.; Meinhold, R. H.; Sherriff, B. L.; Xu, Z. *J. Mater. Chem.* **1993**, *3*, 1263–1269.
(13) Hibino, T.; Tsunashima, A. *Chem. Mater.* **1998**, *10*, 4055–4061.
(14) Stanimirova, T. S.; Kirov, G.; Dinolova, E. *J. Mater. Sci. Lett.* **2001**, *20*, 453–455.
(15) Lima, E.; Lasperas, M.; de Menorval, L. C.; Tichit, D.; Fajula, F. *J. Catal.* **2004**, *223*, 28–35.
(16) Wang, S.; Alekseev, E. V.; Diwu, J.; Casey, W. H.; Phillips, B. L.; Depmeier, W.; Albrecht-Schmitt, T. E. *Angew. Chem., Int. Ed.* **2010**, *49*, 1057–1060.
(17) Joo, S. H.; Choi, S. J.; Oh, I.; Kwak, J.; Liu, Z.; Terasaki, O.; Ryoo, R. *Nature* **2001**, *412*, 169–172.

rational design of extended frameworks with coordinatively unsaturated metal sites and controlled pore/channel size for size-selective Lewis acidity.

Metal−organic frameworks (MOFs) have received remarkable attention in recent years because of not only their intriguing structures but also their use in gas absorption/storage,[21,22] gas separation,[23,24] and ion exchange.[25,26] As a small subgroup of MOFs, cationic MOFs occur when the positive charge on the metal ions outnumber the negative (or neutral) charge on the organic linkers. The net positive charge on the framework necessitates charge-balancing extra-framework anions.[27−33] Among this group of cationic MOFs, only a few have been investigated for reversible anion exchange.[28,30,32] There has been no investigation of anion pollutant trapping by exchange of organic species for inorganic molecules.

Herein, we report the first cationic MOFs that possess both chemical stability for recyclable heterogeneous catalysis and structural flexibility for reversible anion exchange. The first is a Cu(I)-based cationic MOF similar to our recently reported $Ag_2(4,4'-bipy)_2(O_3SCH_2CH_2SO_3) \cdot 4H_2O$ (SLUG-21).[34] The materials were designed to have weak electrostatic interaction between the interlamellar anions and cationic MOF layers. As a result, both display reversible anion exchange between organosulfonate and various inorganic species. SLUG-21 has also been applied for anion trapping of MnO_4^- and ReO_4^- as a model for pertechnetate, a problematic pollutant.[35] We also report a detailed comparative study of the two materials toward size-selective heterogeneous Lewis acid catalysis.

Experimental Section

Reagents. Silver nitrate (AgNO₃, Fisher, 99%), copper acetate monohydrate [Cu(CH₃COO)₂·H₂O, Alfa-Aesar, 98%], 1,2-ethanedisulfonic acid (HO₃SCH₂CH₂SO₃H, TCI Inc., 95%), and 4,4′-bipyridine [(C₅H₄N)₂, Acros Organics, 98%] were used as-received for the synthesis. Sodium nitrate (NaNO₃, Fisher, 99%), sodium perchlorate monohydrate (NaClO₄·H₂O, Fluka Analytical, 98%), potassium permanganate (KMnO₄, Fisher, 99.8%), potassium perrhenate (KReO₄, Acros Organics, 99%), and 1,2-ethanedisulfonic acid disodium salt (NaO₃SCH₂CH₂SO₃Na, TCI Inc., 95%) were used as-purchased for the reversible anion exchange reactions. 2-Butanone (CH₃COCH₂CH₃, Acros Organics, 99%), 2-pentanone (CH₃COCH₂CH₂CH₃, TCI America, 97%), benzophenone (C₆H₅COC₆H₅, Alfa-Aesar, 99%), ethylene glycol (HOCH₂CH₂OH, Acros Organics, 99%), and toluene (C₆H₅CH₃, Fisher, 99.7%) were used as-purchased for the catalytic studies.

Synthesis. Yellow-brown crystals of Cu₂(4,4′-bipy)₂-(O₃SCH₂CH₂SO₃)·3H₂O (which we denote SLUG-22: University of California, Santa Cruz, structure no. 22) were synthesized under hydrothermal conditions. A mixture of Cu(CH₃COO)₂·H₂O (0.27 g, 1.35 mmol), HO₃SCH₂CH₂SO₃H (0.29 g, 1.52 mmol), 4,4′-bipyridine (0.21 g, 1.34 mmol), and 10 mL of water was stirred at room temperature for 10 min and then transferred to a 15 mL Teflon lined autoclave to 2/3 filling. The autoclaves were heated at 175 °C for 4 days under autogenous pressure, followed by slow cooling at a rate of 6 °C/h to room temperature. During the reaction, the pH slightly decreased from 4.1 to 3.5. Yellow-brown block crystals were isolated after filtration and rinsed with water and acetone (yield: 0.46 g, 95% based on copper acetate). IR (KBr pellets): 3467s (O−H stretch), 3050m (aromatic C−H stretch); 1605s, 1535s, 1490s, 1418s (aromatic C=C and C=N stretch); 1328s (CH₂ stretch); 1200m, 1070m (SO₃ stretch); 863s, 817s (aromatic C−H bending).

Colorless crystals of SLUG-21 were synthesized under hydrothermal conditions or at room temperature as previously reported.[34] A reactant solution with a molar ratio of 1:1:1:400 for AgNO₃/EDSA/4,4′-bipy/H₂O were placed into a 15 mL Teflon-lined autoclave to 2/3 filling and heated at 150 °C for 5 days under autogenous pressure. For both compounds, the product was filtered, rinsed with acetone, and allowed to air-dry.

Anion Exchange. 100 mg of either SLUG-21 (0.126 mmol) or SLUG-22 (0.147 mmol) solid were placed into 20 mL of 0.1 M NaNO₃ or NaClO₄ solution and allowed to react either statically for 7 days or with mild stirring for 1 to 3 days. The exchange solution and solid were monitored at various time intervals to follow the exchange progress. The crystal products were isolated by filtration and rinsed with water/acetone. The crystals after NaNO₃ or NaClO₄ exchange were placed into excess 0.1 M EDS disodium salt solution. The mixture was gently stirred for 3 days, followed by filtration to isolate the solid product and exchange solution after the second exchange. The entire process was repeated several times.

Heterogeneous Catalysis. Ketal formation with various substrates was used to characterize the performance of both SLUG-21 and SLUG-22 as a Lewis acid catalyst. 100 mg of the as-synthesized catalyst, 70 mmol of ketone (2-butanone, 2-pentanone or benzophenone), and 70 mmol of ethylene glycol were introduced into 80 mmol of toluene, the latter used as a solvent. The reaction was refluxed at 110 °C under Dean−Stark conditions for 12 h and/or 24 h. The catalyst was isolated by filtration and reused on subsequent runs without further treatment. All product yields were determined by ¹H NMR (Supporting Information).

Instrumental Details. Samples for powder X-ray diffraction (PXRD) were measured on a Rigaku Americas Miniflex Plus diffractometer and were scanned from 2° to 60°(2θ) at a rate of 2° per minute and 0.04° step size under Cu Kα radiation ($\lambda = 1.5418$ Å). Single-crystal X-ray diffraction data for SLUG-22 were collected at Beamline 11.3.1 at the Advanced Light Source (ALS), Lawrence Berkeley National Laboratory ($\lambda = 0.77490$ Å). The structure was solved by direct methods and refined with SHELX-TL.[36] The models were refined by full-matrix least-squares analysis of F^2 against all reflections. All non-hydrogen atoms were refined with anisotropic thermal displacement parameters. Crystal structure views were obtained using Diamond v3.2 and rendered by POV-Ray v3.6. Thermogravimetric analysis (TGA) was performed using

(18) Lee, J.; Farha, O. K.; Roberts, J.; Scheidt, K. A.; Nguyen, S. T.; Hupp, J. T. *Chem. Soc. Rev.* **2009**, *38*, 1450.

(19) Swanson, C. H.; Shaikh, H. A.; Rogow, D. L.; Oliver, A. G.; Campana, C. F.; Oliver, S. R. J. *J. Am. Chem. Soc.* **2008**, *130*, 11737−11741.

(20) Horike, S.; Dincă, M.; Tamaki, K.; Long, J. R. *J. Am. Chem. Soc.* **2008**, *130*, 5854−5855.

(21) Chae, H. K.; Siberio-Perez, D. Y.; Kim, J.; Go, Y.; Eddaoudi, M.; Matzger, A. J.; O'Keeffe, M.; Yaghi, O. M. *Nature* **2004**, *427*, 523−527.

(22) Murray, L. J.; Dincă, M.; Long, J. R. *Chem. Soc. Rev.* **2009**, *38*, 1294−1314.

(23) Wang, B.; Côté, A. P.; Furukawa, H.; O'Keeffe, M.; Yaghi, O. M. *Nature* **2008**, *453*, 207−211.

(24) Banerjee, R. P., A.; Wang, B.; Knobler, C.; Furukawa, H.; O'Keeffe, M.; Yaghi, O. M. *Science* **2008**, *319*, 939−943.

(25) Oliver, S. R. J. *Chem. Soc. Rev.* **2009**, *38*, 1868−1881.

(26) Custelcean, R.; Moyer, B. A. *Eur. J. Inorg. Chem.* **2007**, 1321−1340.

(27) Yaghi, O. M.; Li, H. L.; Groy, T. L. *Inorg. Chem.* **1997**, *36*, 4292−4293.

(28) Min, K. S.; Suh, M. P. *J. Am. Chem. Soc.* **2000**, *122*, 6834−6840.

(29) Sudik, A. C.; Cote, A. P.; Yaghi, O. M. *Inorg. Chem.* **2005**, *44*, 2998−3000.

(30) Du, M.; Zhao, X. J.; Guo, J. H.; Batten, S. R. *Chem. Commun.* **2005**, 4836−4838.

(31) Bao, S. S.; Ma, L. F.; Wang, Y.; Fang, L.; Zhu, C. J.; Li, Y. Z.; Zheng, L. M. *Chem.−Eur. J.* **2007**, *13*, 2333−2343.

(32) Michaelides, A.; Skoulika, S. *Cryst. Growth Des.* **2009**, *9*, 2039−2042.

(33) Chen, X. D.; Wan, C. Q.; Sung, H. H. Y.; Williams, I. D.; Mak, T. C. W. *Chem.−Eur. J.* **2009**, *15*, 6518−6528.

(34) Fei, H.; Paw U, L.; Rogow, D. L.; Bresler, M. R.; Abdollahian, Y. A.; Oliver, S. R. J. *Chem. Mater.* **2010**, *22*, 2027−2032.

(35) Wang, Y.; Gao, H. *J. Colloid Interface Sci.* **2006**, *301*, 19−26.

(36) *SHELXTL Crystal Structure Determination Package*; Bruker Analytical X-ray Systems Inc.: Madison, WI, 1995−99.

Table 1. Crystallographic Information, Data Collection, and Refinement Parameters for SLUG-22

|	
empirical formula	$Cu_2C_{22}H_{26}O_9N_4S_2$
formula weight (g·mol^{-1})	681.71
temperature (K)	150(2)
wavelength (Å)	0.774 90 (synchrotron)
crystal system	triclinic
space group	$P\bar{1}$
unit cell dimensions	$a = 8.9031(9)$ Å　　$b = 10.9120(11)$ Å
	$c = 14.4304(10)$ Å　$\alpha = 103.6150(10)°$
	$\beta = 102.272(2)°$　$\gamma = 97.5290(10)°$
volume (Å^3)	1307.0(2)
Z	2
crystal descriptions	yellow block
crystal size (mm^3)	$0.05 \times 0.04 \times 0.04$
index range	$-11 \leq h \leq 11, -13$
	$\leq k \leq 13, -18 \leq l \leq 18$
density (calculated g·cm^{-3})	1.732
reflections collected	14355
unique reflections	5316
final R indices [$I > 2\sigma(I)$]	$R_1 = 0.0371, wR_2 = 0.0957$
R indices (all data)	$R_1 = 0.0500, wR_2 = 0.1021$
largest diff. peak and hole	-0.63 and 0.67 e$^-$·Å^{-3}
goodness of fit on F^2	1.037

a TA Instruments 2050 TGA by heating from 30 to 700 °C under a N$_2$ purge with a gradient of 15 °C/min. *In situ* mass spectra coupled to the TGA were collected on a Pfeiffer Vacuum ThermoStar GSD 301 T3 mass spectrometer with a 70 eV ionization potential. UV−vis spectroscopic studies were collected on a Hewlett-Packard Model 8452A spectrophotometer to monitor the exchange progress. Fourier transform infrared (FTIR) spectroscopy of the materials was collected on a Perkin-Elmer Spectrum One spectrophotometer with KBr pellets. ^{1}H NMR spectra were collected with a Varian Oxford 600 MHz spectrometer by dissolving the sample in 700 μL of deuterated choloroform with tetramethylsilane as an internal standard.

Results and Discussion

Synthesis. Yellow block crystals of SLUG-22 were obtained hydrothermally as a pure phase and in high yield at 175 °C and pH ≈ 4.1. A lower temperature (125 or 150 °C) or slight change in the pH led to lower crystallinity and an unidentified impurity in the product that could be observed by optical microscopy. During the hydrothermal synthesis, the Cu(II) reagent was reduced to Cu(I), as observed by the color change between the copper precursor and product. Unlike SLUG-21, the material cannot be synthesized at room temperature or reflux conditions, and nonaqueous solvents were unsuccessful. The synthesized product was insoluble in water, acetone, ethanol, and other common organic solvents.

Structure Characterization. SLUG-22 crystallizes in a triclinic system with a $P\bar{1}$ space group (Table 1), which is the same as our previous reported SLUG-21 structure. Synchrotron single-crystal X-ray diffraction studies reveal that the structure of SLUG-22 is also a cationic one-dimensional MOF with infinite chains composed of alternating copper(I) centers and 4,4′-bipy organic linkers (Figures 1 and 2). The Cu(I)−bipy chains are arranged into close-packed layers by π−π stacking between adjacent 1D chains (Figure 2, right). The Cu(I) atoms and its full d shell form an almost linear two-coordinate environment, with N(5)−Cu(3)−N(6) and N(7)−Cu(4)−N(8) angles between 169.40(11)° and 169.48(11)°.

The distance between the adjacent Cu(I)−bipy chains is *ca.* 3.466 Å, which is in the reasonable range of π−π stacking distance,[37] leading to a cationic layer. Only one oxygen of the interlamellar EDS anions has a weak interaction toward Cu(I), with distances in the range of 2.434(2) to 2.501(2) Å (Figure
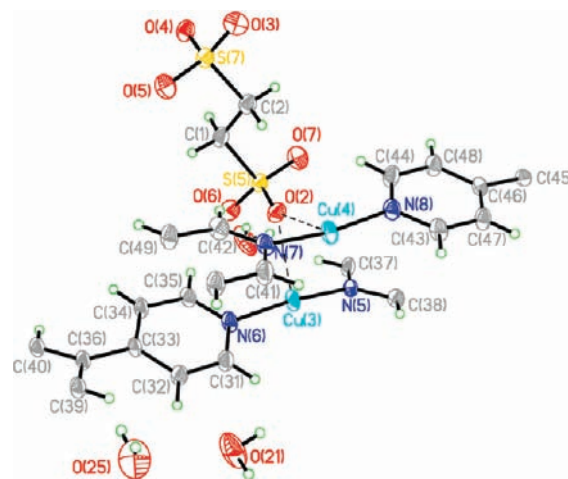
Figure 1. ORTEP diagram and atomic labeling of SLUG-22. Thermal ellipsoids are shown at 50% probability.

1). The *Cambridge Crystal Structure Database* indicates the median bond length of Cu(I)−O is 1.978 Å.[38] The literature bond length values between Cu(I) and a sulfonate oxygen are 2.03 to 2.22 Å,[39−41] further supporting only weak electrostatic interaction between the cationic Cu(I)-bipy framework and the charge-balancing EDS anion. This feature is important for the anion exchange and catalytic properties of the material that will be discussed below.

Thermal Properties. The thermal stability of SLUG-22 was investigated by TGA under a N$_2$ purge and *ex situ* PXRD (Figures 3 and S3, Supporting Information, respectively). The TGA trace of SLUG-22 indicates a slight mass loss of ∼3% at *ca.* 70 °C, likely due to partial loss of the interlamellar water (observed: 3.1%; calculated: 7.9%, Figure 3). In agreement with the loss of the crystallographic water is a slight structural transformation observed by *ex situ* PXRD. This structure is stable to *ca.* 325 °C, when both 4,4′-bipyridine and ethanedisulfonate ligands in the structure start to decompose. This gradual mass loss leads to metallic copper at *ca.* 450 °C (observed: 17.8%; calculated: 18.8%). *Ex situ* PXRD under a N$_2$ flow also confirms the formation of pure phase Cu (PDF# 71-3761) above 450 °C. The slight mass increase from 450 to 490 °C is presumably due to nitrogen uptake.

Anion Exchange. Considering that both SLUG-22 and our previously reported SLUG-21 have only one oxygen of the EDS weakly interacting with the cationic metal−bipy layers, the materials were investigated systematically for reversible anion exchange. Many previously reported cationic inorganic materials can only exchange its extra-framework anions for smaller or similar sized inorganic anions. For example, Yu et al. reported Cl$^-$ located in a microporous aluminoborate framework can be partially exchanged by Br$^-$.[42] A similar phenomenon is observed for the 2-D metal oxychloride francisite and its derivatives.[43] As mentioned earlier, coordination polymers have been inves-

(37) Lucassen, A. C. B.; Karton, A.; Leitus, G.; Shimon, L. J. W.; Martin, J. M. L.; van der Boon, M. E. *Cryst. Growth Des.* **2007**, *7*, 386−392.

(38) Cambridge Crystal Structure Database; 8022 of 8818 (91%) Cu(I)−O bonds with a bond length less than 2.439 Å, and mean bond length is 2.090 Å with standard deviation of 0.213 Å.

(39) Wu, M. Y.; Yuan, D. Q.; Han, L.; Wu, B. L.; Xu, Y. Q.; Hong, M. C. *Eur. J. Inorg. Chem.* **2006**, 526−530.

(40) Ju, J.; Lin, J. H.; Li, G. B.; Yang, T.; Li, H. M.; Liao, F. H.; Loong, C. K.; You, L. P. *Angew. Chem., Int. Ed.* **2003**, *42*, 5607−5610.

(41) Liu, S. X.; Xie, L. H.; Gao, B.; Zhang, C. D.; Sun, C. Y.; Li, D. H.; Su, Z. M. *Chem. Commun.* **2005**, 5023−5025.
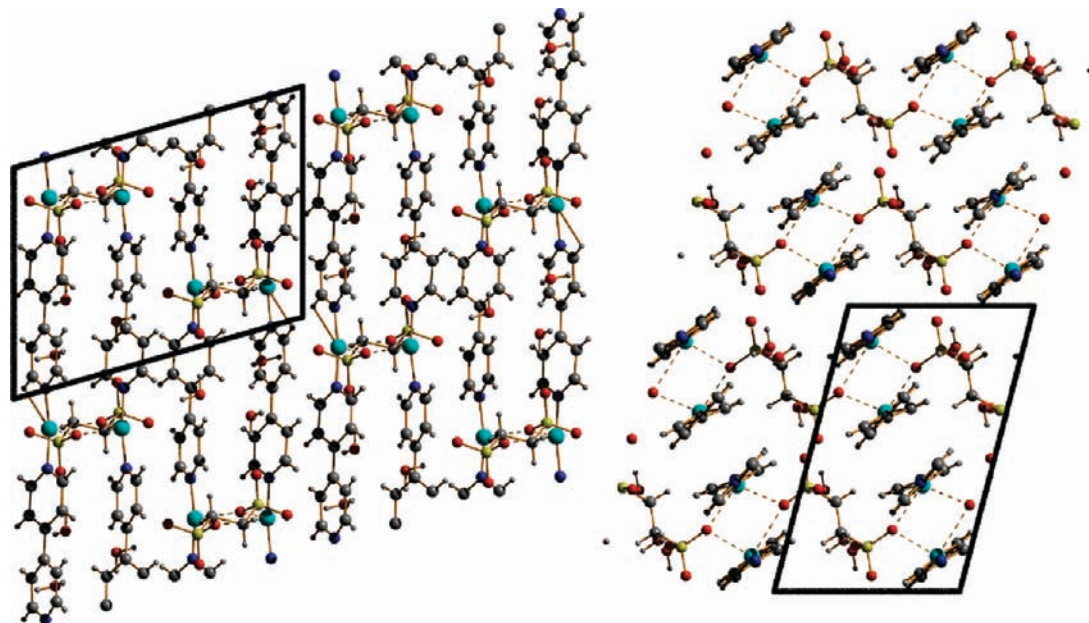
Figure 2. Crystallographic *a*-projection (left) and *b*-projection (right) of the SLUG-22 structure (copper: green; carbon: gray; sulfur: yellow; oxygen: red; nitrogen: blue).
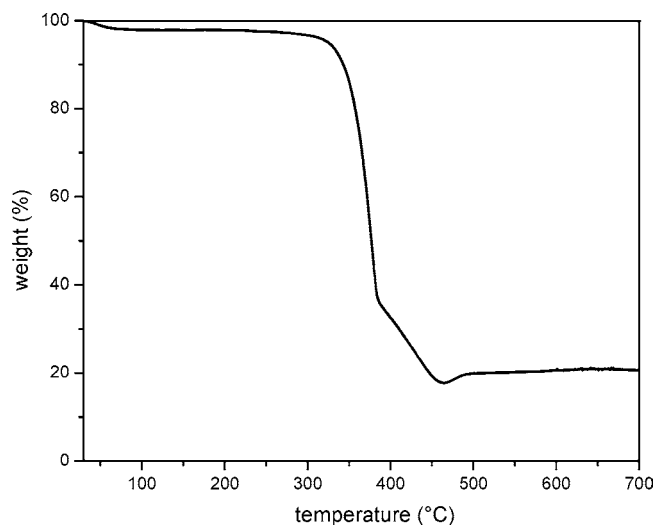

Figure 3. Thermogravimetric analysis of SLUG-22 in the range of 30 to 700 °C.

tigated for reversible/irreversible anion exchange, including extra-framework NCS^-, N_3^-, NO_3^-, Cl^-, $CF_3SO_3^-$, and/or ClO_4^-.[28,30,32] Meanwhile, there have been no reports of exchange of bulky organic anions for inorganic species aside from the LDHs/hydrotalcites, which have limited reusability and anion uptake.

As initial examples of exchange, we have focused on several inorganic anions for two reasons: (i) the oxo-anions of many metals are EPA priority pollutants; (ii) nitrate and perchlorate were successful templates for our previously reported cationic lead fluoride structures.[44,45] Figure 4 shows the FTIR and PXRD of the solid products after exchange of the EDS in SLUG-21 for nitrate. The four singlet bands at 1605, 1535, 1490, and 1418 cm^{-1} are aromatic C=C and C=N bending, confirming

the presence of 4,4′-bipy throughout the exchange, as expected. The strong, broad band at ∼1200 cm^{-1} is characteristic of the SO_3^- group, confirming the presence of EDS anions in the initial SLUG-21 framework (Figure 4a, black spectrum). By simply immersing as-synthesized SLUG-21 crystals in 0.1 M NaNO$_3$ solution at room temperature with mild stirring, both FTIR and PXRD indicate the EDS anions in SLUG-21 were completely exchanged for NO_3^- after 3 days (Figure 4b, red spectra, 1330 cm^{-1}). The broad ∼1200 cm^{-1} band has disappeared, with a new peak at ∼1330 cm^{-1} characteristic of NO_3^- (N—O stretch).

PXRD further supports a complete, reversible exchange between EDS and nitrate. Although the exchanged product could not be solved by X-ray crystallography due to lower crystal quality (Figure S2), the resultant PXRD pattern after 3 days corresponds exactly to the theoretical pattern of the previously reported Ag(4,4′-bipy)NO$_3$.[46] The first peak is at a higher angle, as expected for replacement of the larger EDS anions for the smaller nitrate molecules. The layer-to-layer distance decreased from *ca.* 4.6 Å to *ca.* 3.0 Å, with long Ag—Ag contact between the layers [*ca.* 2.976(2) Å] and the nitrates between adjacent Ag-bipy chains The bipyridine rings have thus "shuttered" upon nitrate intercalation, favoring interlayer π—π stacking. Simply immersing the nitrate exchanged product into a 0.1 M EDS disodium salt aqueous solution reforms the original SLUG-21, confirmed by both FTIR and PXRD (Figure 4c, blue spectra) The reversibility implies that the bulky alkanesulfonate anions favor a more open framework with stronger intralayer π—π stacking. Indeed, SLUG-21 forms during the synthesis rather than Ag(4,4′-bipy)NO$_3$ despite the fact that silver nitrate was the synthetic reagent. In fact, SLUG-21-NO$_3$ reforms SLUG-21 when placed into a mixed aqueous solution of 0.1 M EDS disodium salt and 0.1 M NaNO$_3$, an analogous anionic mixture compared to the synthetic procedure. Based on these observations, we conclude that the SLUG-21 exchange reaction with

(42) Yu, J. H.; Xu, R. R.; Chen, J. S.; Yue, Y. *J. Mater. Chem.* **1996**, *6*, 465–468.

(43) Ok, K. M.; Halasyamani, P. S. *Inorg. Chem.* **2002**, *41*, 3805–3807.
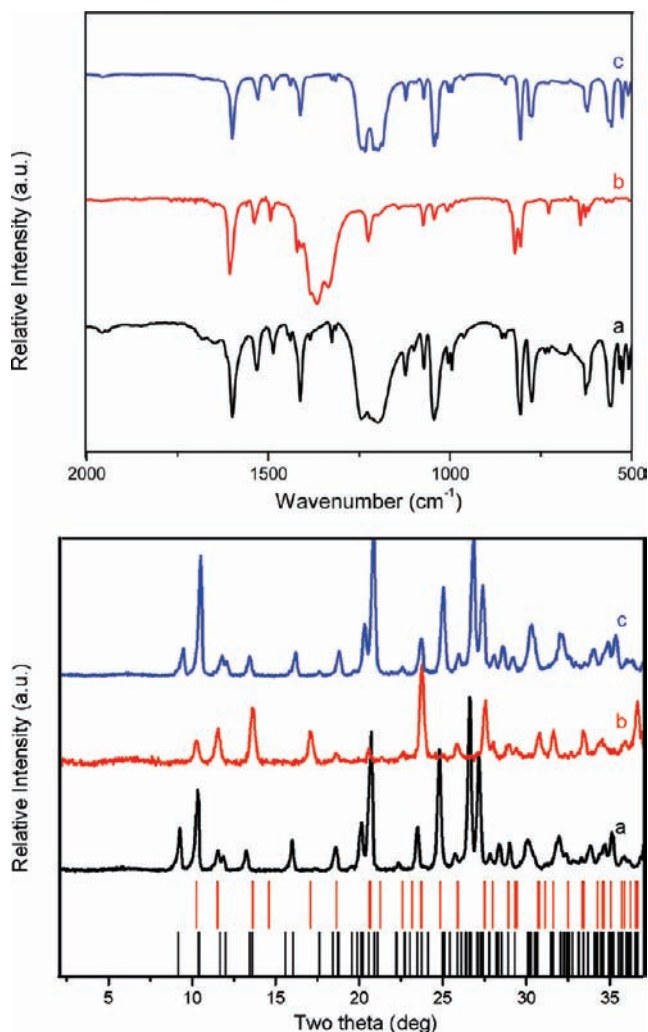
(44) Tran, D. T.; Zavalij, P. Y.; Oliver, S. R. J. *J. Am. Chem. Soc.* **2002**, *124*, 3966–3969.

(45) Rogow, D. L.; Russell, M. P.; Wayman, L. M.; Swanson, C. H.; Oliver, A. G.; Oliver, S. R. J. *Cryst. Growth Des.* **2010**, *10*, 823–829.

(46) Yaghi, O. M.; Li, H. L. *J. Am. Chem. Soc.* **1996**, *118*, 295–296.

Figure 4. FTIR (top) and PXRD (bottom) of (a) SLUG-21 (black); (b) the solid product after 3 days exchange reaction between SLUG-21 and 0.1 M NaNO$_3$ ("SLUG-21-NO$_3$", red); and (c) the solid product after 3 days exchange reaction between "SLUG-21-NO$_3$" and 0.1 M EDS sodium salt solution (blue). Theoretical PXRD patterns of SLUG-21 (black) and SLUG-21-NO$_3$ (red) are shown as bars in the bottom figure.

nitrate is concentration induced rather than a stronger interaction between the cationic framework and anion. The large hydration energy of nitrate also likely aids in the reversibility.

In addition to reversible exchange with nitrate, SLUG-21 exhibits analogous chemistry with perchlorate. FTIR and PXRD (Figure S2, Supporting Information) indicate that perchlorate anions intercalate into the cationic layered framework, releasing EDS and resulting in the previously reported phase Ag(4,4′-bipy)ClO$_4$.[47] The structure is again a cationic layer where again the interlayer distance decreased due to the smaller anion size, closer interaction to the anion [*ca.* 3.913(4) Å], and shuttering of the Ag−bipy chains to give interlayer $\pi-\pi$ stacking.

As a final illustration of anion exchange capability, we investigated SLUG-21 for permanganate and perrhenate trapping. These anions were chosen as models for pertechnetate, a problematic radioactive pollutant. The trapping was monitored versus time by optical microscopy and UV−vis spectroscopy. Figure 5 shows the *in situ* optical microscopy of the anion

(47) Wang, L. S.; Zhang, J. F.; Yang, S. P. *Acta Crystallogr., Sect. E* **2004**, *E60*, m1484−m1486.

exchange between an individual crystal of SLUG-21 and stoichiometric excess 1.26 mM aqueous permanganate solution. A visible color change of both crystals (more were present outside the image area) and surrounding solution occurred in 10 min. The permanganate anions can be seen diffusing into the structure from the left after 15 min of immersion (Figure 5). No apparent morphology change occurred after immersion of the crystals in solution for 1 h. The crystals after exchange again could not be solved by single crystal X-ray diffraction due to reduction in crystallinity. Nevertheless, the crystals retain their morphology throughout, and the anion exchange reaction is therefore a solid-state process.

A series of UV−vis patterns were collected on the permanganate solution during the anion exchange process (Figure 6). In this case, a stoichiometric excess of 150 mg of as-synthesized SLUG-21 crystals was placed into 50 mL of 1.26 mM permanganate solution; the mixture was stirred mildly for 5 min before UV−vis data collection to ensure homogeneity. To determine percent exchange, UV−vis spectra were also collected of a saturated KMnO$_4$ solution, diluting from 1 to 5 mL with deionized water. Based on Beer's Law, 36.8%, 68.3%, and 100% of the MnO$_4^-$ from the solution were exchanged into SLUG-21 after 8, 24, and 96 h, respectively. The absorption below 280 nm for the 96 h sample is due to EDS, which is now fully exchanged and present in sufficient concentration to absorb. Both crystal morphology and size are unchanged throughout the 4 day anion exchange. SLUG-21 remains heterogeneous at the bottom of the solution and can be readily recovered after exchange.

PXRD before and after the exchange reaction confirms that no AgMnO$_4$ phase formed (bars in Figure 7). Instead, the new SLUG-(change 22 to 21)-MnO$_4$ phase is highly crystalline, with a shift of both (010) and (001) peaks to a higher angle (the *d*-spacing decreases from *ca.* 9.63 and 8.50 Å to 7.49 and 8.25 Å, respectively). Since the ethanedisulfonate anions are oriented in the [101] direction, the lattice has contracted along both the *b* and *c* axes, presumably due to the difference in anion size/shape between permanganate and ethanedisulfonate. No known structure exists based on Ag−bipy and permanganate, nor was single crystal analysis possible. FTIR before and after anion exchange (Figure S4, Supporting Information), however, confirms the presence of the Ag−bipy framework, while the sulfonate peaks were completely replaced by permanganate peaks. Although exchange of Ag−bipy−MnO$_4$ for EDS was unsuccessful, the permanganate anions can be trapped, with selectivity: SLUG-21 in a mixed solution of both permanganate and nitrate (0.1 M each) preferably reacts with permanganate, leading to the same phase as that above using pure permanganate solution. These data indicate that the permanganate pollutant trapping is based on a stronger interaction between MnO$_4^-$ and the SLUG-21 cationic framework, which would also account for the lack of reversibility for permanganate exchange. In addition to solid-state anion pollutant trapping with permanganate, SLUG-21 display analogous chemistry with perrhenate, as determined by FTIR and PXRD (Figure S5, Supporting Information). The material may therefore find application as a pertechnetate trapping material.

SLUG-22 was also employed in the same exchange reaction with nitrate and perchlorate to obtain structure−property insight. The structure is similar to SLUG-21, so we wished to understand if this anion exchange property is common for the bipy polymers of d^{10} group 11 metals. The characteristic absorption of nitrate in the UV region at 305 nm was followed since EDS has no absorption at wavelengths longer than 240 nm. Progression of
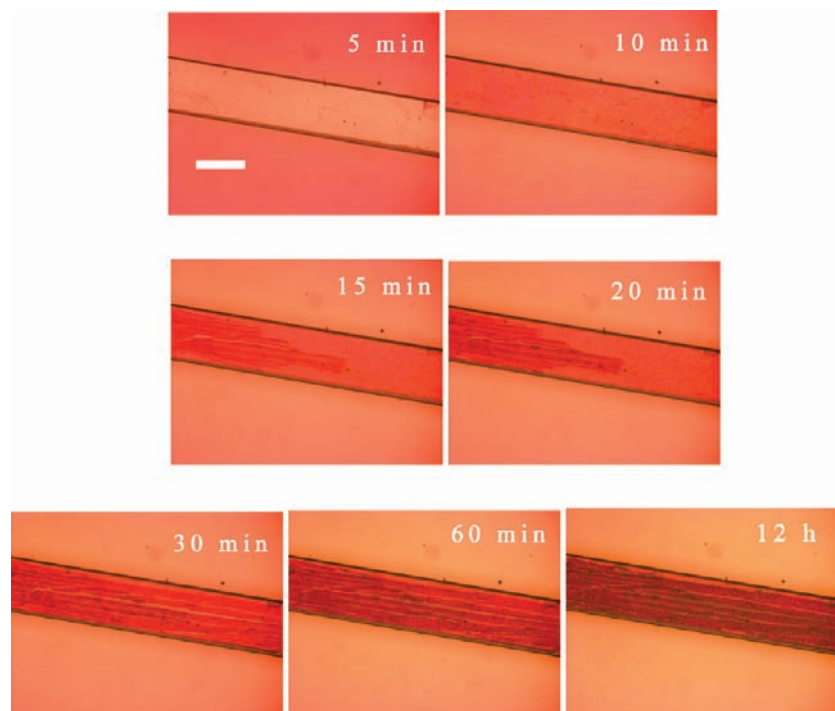
Figure 5. Optical micrographs of SLUG-21 crystals in permanganate solution versus time (scale bar: 500 μm).
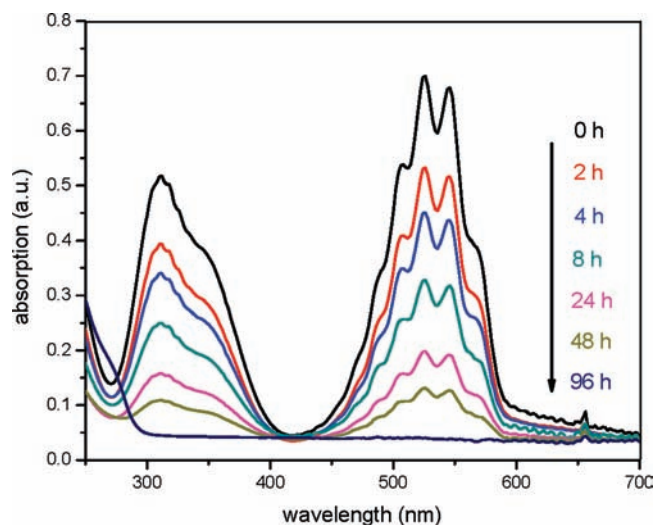

Figure 6. UV−vis spectra of the permanganate solution during anion exchange with SLUG-21 at various time intervals, showing complete exchange for EDS.
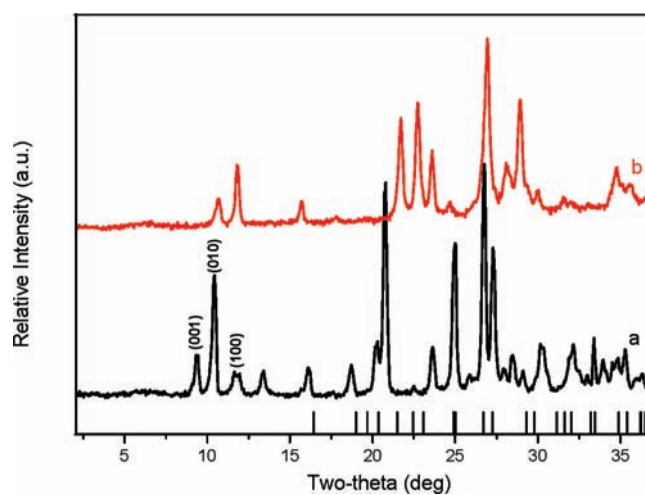

Figure 7. PXRD of (a) as-synthesized SLUG-21 and (b) SLUG-21 after exchange with excess permanganate after 4 days. Theoretical pattern of $AgMnO_4$ is shown as bottom bars, indicating no structural decomposition occurred during the anion exchange.

UV−vis absorption spectra for anion exchange of SLUG-22 in sodium nitrate solution was carried out for 3 days (Figure 8). Nitrate was added in 50% molar excess (1.0 mmol SLUG-22 in 1.5 mmol nitrate solution), and SLUG-22 exhibits highly efficient anion exchange with over 90% exchange (based on SLUG-22) after 1 day, forming the previously reported structure.[48] EDS could be reintroduced, giving rise to the partially dehydrated material mentioned above, obtained after heating SLUG-22 to 70 °C (Figure S3, Supporting Information). In addition to nitrate, SLUG-22 also displayed reversible anion exchange with perchlorate (Figure 9). Similar to the SLUG-21 exchange reaction above, FTIR shows the disappearance of the broad absorbance peak at ∼1200 cm^{-1} and singlet band at 1020

cm^{-1} (sulfonate stretching) after 3 days of exchange reaction. The appearance of a strong broad band at ∼1100 cm^{-1} confirms that the perchlorate has exchanged with EDS, again forming a previously reported structure,[49] with complete reversibility after subsequent exchange in EDS solution.

Size-Selective Heterogeneous Catalysis. In addition to the excellent anion exchange properties of SLUG-21 and SLUG-22, both compounds are highly stable in common organic solvents. We then found these two materials are catalytically active in heterogeneous ketal formation. Ketalization is an important method to protect carbonyl groups in organic synthesis

(48) Yaghi, O. M.; Li, H. *J. Am. Chem. Soc.* **1995**, *117*, 10401–10402.

(49) Zhang, J.; Kang, Y.; Wen, Y.; Li, Z.; Qin, Y.; Cheng, J.; Yao, Y. *Acta Crystallogr., Sect. E* **2004**, *E60*, m504–m505.
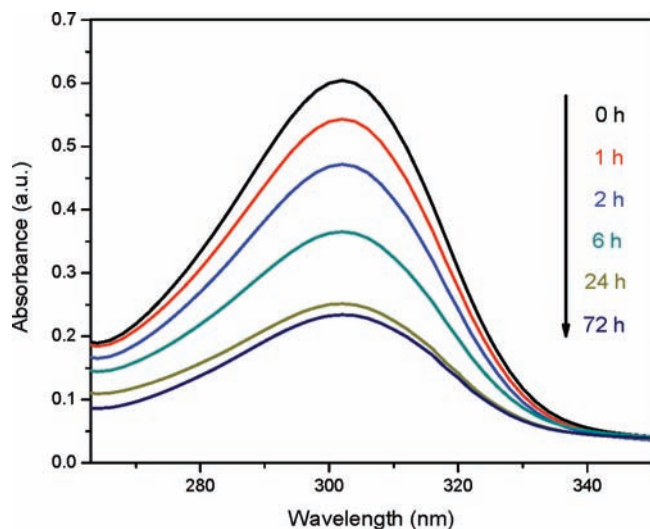
Figure 8. UV−vis absorption spectra of the anion exchange solution for SLUG-22 and nitrate.
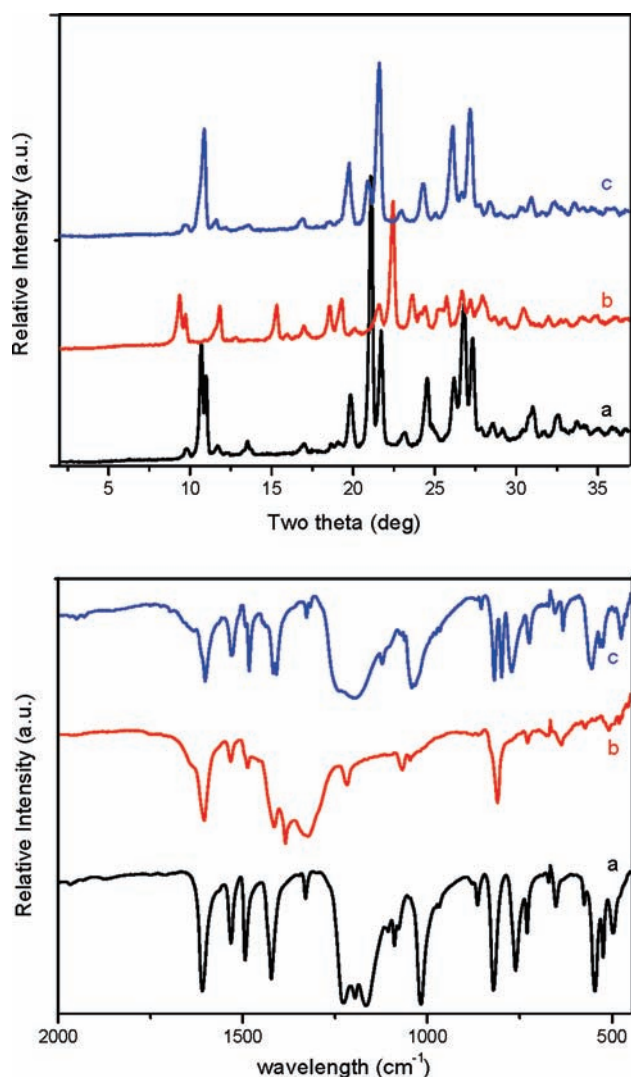

Figure 9. PXRD (top) and FTIR (bottom) of (a) SLUG-22 (black); (b) the solid product after 3 days exchange reaction between SLUG-22 and 0.1 M NaClO₄ (SLUG-22-ClO₄, red); and (c) the solid product after 3 days exchange reaction between SLUG-22-ClO₄ and 0.1 M EDS sodium salt solution (blue).

Scheme 1. Acid Catalyzed Ketal Formation between 2-Butanone and Ethylene Glycol
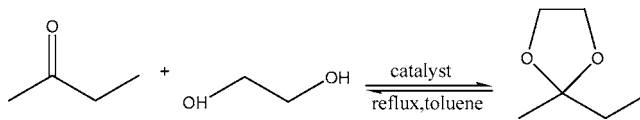

Table 2. Conversion Yields for the Ketalization of 2-Butanone

catalyst	number of run	time (h)	conv. (%)[a]
SLUG-21	run #1	12	97
	run #2	12	96
	run #3	12	95
SLUG-22	run #1	12	93
	run #2	12	72
	run #3	12	71

[a] Conversion yields were determined by ¹H NMR.

and drug design.[50] The reaction requires a Lewis acid catalyst to activate the oxygen of the carbonyl group, allowing glycol to substitute the ketone group. The reaction typically uses homogeneous iodine or toluenesulfonate, in 56−94% yield.[50]

Both structures as-prepared display heterogeneous Lewis acidity and reusability in activating 2-butanone to form 2-ethyl-2-methyl-[1,3]-dioxolane (Scheme 1, Table 2). Unlike the conventional homogeneous catalyst, both SLUG-21 and SLUG-22 are heterogeneous and easily separated from the product. The catalyst can be reused without further treatment after catalytic runs. Removal of either catalyst by filtration after a 6 h reaction time gave only a 2% increase in yield after an additional 6 h of reflux. This observation confirms that the catalysis is heterogeneous, with no leaching of a homogeneously active species into the reaction solution. In addition, the sulfonate is retained by the material, as confirmed by postcatalysis FTIR of the solid. SLUG-21 shows almost no decrease in yield after additional runs, while SLUG-22 showed a decrease in yield from 93% to 72% for the second run and 71% for the third. Extending the reaction time from 12 to 24 h did not enhance the conversion efficiency. PXRD of the postcatalysis SLUG-22 material shows a transformation occurred, with a shift of the (10−1) and (20−2) peaks to a lower angle (Figure 10). This expansion of the lattice is possibly due to reorientation of the EDS anions (Figure 2) and bonding to the Ag centers to reduce catalytic activity. Nevertheless, this activated form of SLUG-22 is stable under these conditions, retaining its crystallinity in spite of the lower ketal yield.

We also investigated the size selectivity of the catalyst for ketone precursor, to determine whether the reactions are occurring in the channels of the relatively open interlayer space (Figure 2) or on the crystal surface. Ketalization of 2-butanone, 2-pentanone, and benzophenone by ethylene glycol were performed for both SLUG-21 and SLUG-22 (Table 3). A significant size selectivity was observed for SLUG-21: the more bulky benzophenone led to a yield of only 31%, less than one-third that of 2-butanone. This result demonstrates that ketal formation by SLUG-21 is likely occurring primarily in the 1D pore channels along the *b*-axis.[34] The relative dimensions indicate that the cross-sectional channel area of SLUG-21 (*ca.* 4.1 Å × 3.7 Å) is large enough to accommodate both 2-butanone (*ca.* 3.5 Å × 1.6 Å × 5.1 Å) and 2-pentanone (*ca.* 3.8 Å × 1.8 Å × 6.8 Å). In contrast, benzophenone (*ca.* 7.8 Å × 5.2 Å ×

(50) Banik, B. K.; Chapa, M.; Marquez, J.; Cardona, M. *Tetrahedron Lett.* **2005**, *46*, 2341–2343.
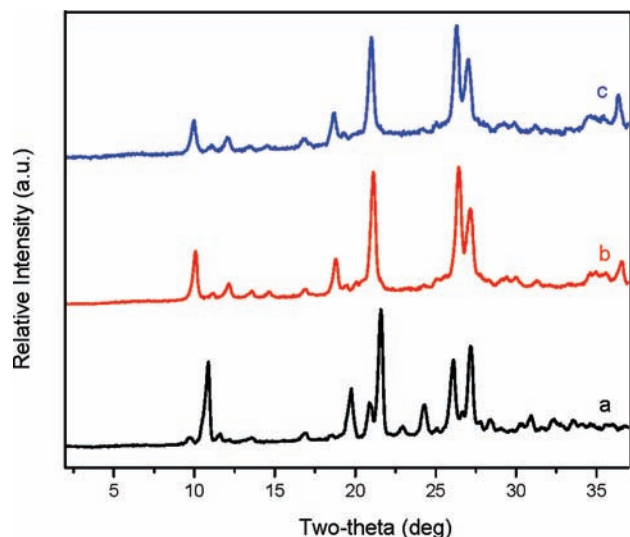
Figure 10. PXRD of SLUG-22: (a) as-synthesized; postcatalysis after one (b) and three (c) catalytic cycles of ketal formation.

Table 3. Conversion Yields for the Ketalization of Larger Substrates

catalyst	ketone precursor	time (h)	conv. (%)[a]
no catalyst	2-butanone	12	1
	2-pentanone	12	0
	benzophenone	12	0
SLUG-21	2-butanone	12	97
	2-pentanone	12	87
	benzophenone	12	31
SLUG-22	2-butanone	12	89
	2-pentanone	12	91
	benzophenone	12	91

[a] Conversion yield is determined by ¹H NMR.

4.6 Å) is too bulky to diffuse into the 1D channel. Meanwhile, no size selectivity was observed for SLUG-22: all three ketone precursors formed in similar yields, indicating that SLUG-22 catalysis likely occurs on the crystal surface. Even so, these yields are still higher than in the case of the conventional homogeneous iodine.[50,51]

Based on these heterogeneous catalytic results, we investigated whether the structural differences between the two frameworks might be responsible for the varying ketalization mechanism and yields. Although both structures possess a similar cationic charge and topology, there are slight structural differences in the EDS anion orientation as well as the position of the crystallographic water. In addition, the silver atoms are larger. The percent solvent/guest accessible void volume was estimated by PLATON.[52] SLUG-21 possesses 16% void space, compared with only 12% for SLUG-22. Moreover, SLUG-21

contains open 1D channels[34] whereas the intercalated water molecules of SLUG-22 are distributed throughout the interlamellar region and should restrict access. Without accessible channels for diffusion of the organic precursor into the structure, surface catalysis would be expected. It is possible that surface Lewis acid sites more easily lose their catalytic activity compared to interior sites due to long-term exposure to the chemical solvent, which would account for the drop in yield versus runs for SLUG-22.

Conclusions

Two Ag(I)/Cu(I)-based cationic metal−organic frameworks have been rationally synthesized using both an organic metal linker and organic structure directing agent. Both materials display efficient anion exchange as well as heterogeneous Lewis acidity. SLUG-21 exhibits reversible anion exchange of its charge-balancing organosulfonate anions for nitrate/perchlorate, as well as a potentially applicable selective solid-state trapping of group(VII) oxometal anions. Although SLUG-22 is not useful for permanganate trapping, likely due to the lower redox stability of Cu(I) versus Ag(I), nitrate and perchlorate can be reversibly exchanged in high percentage. Cationic MOFs are potentially useful for heterogeneous catalysis due to their positive charge compared to the majority of reported MOFs. Our comparative study into the structure−property behavior of two similar extended frameworks on varying substrate size shows that 1-D channels are important in obtaining size-selective, high yield, recyclable heterogeneous catalysts. We are further exploring this two-pronged approach of organic MOF linker and organosulfonate anionic template with other d-block metals to tune the charge density as well as openness, which should further enhance the anion exchange and catalytic properties of cationic MOFs.

Supporting Information Available: Ex situ PXRD, additional anion exchange optical micrographs, FTIR spectra and PXRD pattern of anion exchange between SLUG-21 and perrhenate and permanganate and additional discussion, ¹H NMR spectra, and crystallographic information file (CIF) including refinement parameters and full bond distances. This material is available free of charge via the Internet at http://pubs.acs.org.

JA102134C

(51) Ren, Y. M.; Cai, C. *Tetrahedron Lett.* **2008**, *49*, 7110–7112.

(52) Spek, A. L. *PLATON, A Multipurpose Crystallographic Tool*: Utrecht, The Netherland, 2007.